

# Canonical scale separation in two-dimensional incompressible hydrodynamics

Klas Modin<sup>1</sup> and Milo Viviani<sup>2</sup>

<sup>1</sup>*Department of Mathematical Sciences, Chalmers University of Technology and University of Gothenburg*

<sup>2</sup>*Scuola Normale Superiore, Pisa*

October 16, 2021

## Abstract

Characterization of the long-time behaviour of an invicid incompressible fluid evolving on a two-dimensional domain is a long-standing problem in physics. The motion is described by Euler's equations: a non-linear system with infinitely many conservation laws, yet non-integrable dynamics. In both experiments and numerical simulations, coherent vortex structures, or blobs, typically form after some stage of initial mixing. These formations dominate the slow, large-scale dynamics. Nevertheless, fast, small-scale dynamics also persist. Kraichnan, in his classical work, qualitatively describes a direct cascade of enstrophy into smaller scales and a backward cascade of energy into larger scales. Previous attempts to quantitatively model this double cascade are based on filtering-like techniques that enforce separation from the outset. Here we show that Euler's equations possess a natural, intrinsic splitting of the vorticity function. This canonical splitting is remarkable in four ways: (i) it is defined only in terms of the Poisson bracket and the Hamiltonian, (ii) it characterizes steady flows (equilibria), (iii) it genuinely, without imposition, evolves into a separation of scales, thus enabling the quantitative dynamics behind Kraichnan's qualitative description, and (iv) it accounts for the "broken line" in the power law for the energy spectrum (observed in both experiments and numerical simulations). The splitting originates from a quantized version of Euler's equations in combination with a standard quantum-tool: the spectral decomposition of Hermitian matrices. In addition to theoretical insight, the canonical scale separation dynamics might be used as a foundation for stochastic model reduction, where the small scales are modelled by suitable multiplicative noise.

# 1 Introduction

Consider Euler's equations for a homogeneous, inviscid, and incompressible fluid confined to a two-dimensional surface  $S$ . We shall, in fact, take  $S$  to be the unit sphere  $\mathbb{S}^2$  as it makes our arguments more explicit and enables numerical simulations. However, most concepts are transferable to arbitrary compact surfaces.

In vorticity formulation, Euler's equations on  $\mathbb{S}^2$  are

$$\begin{aligned}\dot{\omega} &= \{\psi, \omega\} \\ \Delta\psi &= \omega,\end{aligned}\tag{1}$$

where  $\omega$  is the vorticity function of the fluid (related to the fluid velocity  $\mathbf{v}$  via  $\omega = \text{curl } \mathbf{v}$ ), and  $\psi$  is the stream function, related to the vorticity function via the Laplace-Beltrami operator  $\Delta$ . The equations (1) constitute an infinite-dimensional Hamiltonian system with an infinite number of conservation laws: total energy

$$H = -\frac{1}{2} \int_{\mathbb{S}^2} \psi \omega dS,$$

linear momentum

$$\mathbf{M} = \int_{\mathbb{S}^2} \mathbf{n} \omega dS,$$

for  $\mathbf{n}$  the normal vector to  $\mathbb{S}^2$ , and Casimir functions

$$C_f(\omega) = \int_{\mathbb{S}^2} f(\omega) dS,$$

for any smooth real function  $f: \mathbb{R} \rightarrow \mathbb{R}$ . These conservation laws are fundamental in describing the long-time behaviour of the fluid, with linear momentum  $\mathbf{M}$ , energy  $H$ , and enstrophy  $C_2 := \int \omega^2$  best understood (see, e.g., Herbert [8]). Using these quadratic invariants, Kraichnan [11, 12] showed that 2D fluids exhibit a double cascade: one towards the small scales, called direct enstrophy cascade, an other towards the large scales, called inverse energy cascade. This phenomenon is crucial in the formation of stable large coherent vortices after an initial turbulent regime. Before Kraichnan, the formation of these condensates was explained by Onsager [16] working with a point vortex model and observing that fluid parcels with same vorticity sign tend to merge and condensate in large blobs. This formations occur because they correspond to states of maximal entropy. Several experimental validations of the theories of Onsager and Kraichnan have been obtained in the last decades [17]. In particular, a major effort has been dedicated in deriving the predicted energy profiles of a 2D fluid for long time simulations [2]. In [4], the characteristic broken line energy profile of a 2D fluid in a periodic box has been

obtained using the wavelet-based vorticity splitting of proposed in [6]. This vorticity splitting characterizes large and small scales in terms of wavelet basis elements, providing a solid strategy in understanding the characteristic energy profile.

However, one of the main limits of this approach is that it is not a canonical choice of what should be considered either large or small scales. Moreover, this choice is determined a priori only considering the enstrophy and the truncation level of the wavelet expansion. Therefore, not much information on the fluid invariants is contained in this choice.

In this paper, we introduce an alternative canonical choice to determine the different fluid scales. Our work is based on the Zeitlin discrete truncation [19] of the 2D fluid on a sphere. We remark that the results here presented can be generalized to any compact surface, considering the analogous Zeitlin model (see [18] for the flat 2-torus, and [3] for the general quantization theory of Poisson bracket on compact manifolds). The advantage in working with the Zeitlin discrete model is that complex topological issues of the Euler equations can be described in terms of linear algebras. Our splitting of the discrete vorticity is both natural and explicit, and it only relies of the eigenvalues decomposition of the discrete stream function. Indeed, we state that the vorticity which describes the large scales is the one on which the action of the stream function is trivial. This splitting has a precise geometric meaning in terms of Lie algebras but also a dynamical interpretation as the steady and unsteady vorticity components. Our scale separation conjecture is demonstrated numerically with a long time simulations. A neat separation of scales in the vorticity energy profile is completely described by our splitting. Furthermore, we determine the dynamics equations for the large and small scales, providing a concrete base for a stochastic model reduction [10]. Finally, we show how to translate our results to the original Euler equations, interpreting the matrix-based results into fluid dynamical ones.

## 2 Quantized Euler equations

In this section, we introduce a discrete model for the Euler equations, first introduced by Vladimir Zeitlin [18, 19]. The model, sometimes called *consistent truncation* or *quantized Euler equations*, relies on the approximation of the infinite dimensional Poisson algebra of the smooth functions on the sphere  $C^\infty(\mathbb{S}^2)$ , where the Poisson bracket  $\{\cdot, \cdot\}$  is determined by the volume form on  $\mathbb{S}^2$ . More explicitly, we have that for any  $p \in \mathbb{S}^2$  and  $f, g \in C^\infty(\mathbb{S}^2)$ :

$$\{f, g\}_p = p \cdot (\nabla f \times \nabla g).$$

It has been shown in [3], that there exists a basis of the Lie algebra  $\mathfrak{su}(N)$ , such that its structure constant converges to those of  $C^\infty(\mathbb{S}^2)$ , expressed in terms of spherical harmonics. More specifically, let  $f, g \in C^\infty(\mathbb{S}^2)$  and let  $Y_{lm}$ , for  $l = 1, \dots, \infty, m = -l, \dots, l$ , be the usual spherical harmonics. Then, for any  $N > 1$ , there exists a basis of  $\mathfrak{su}(N)$ , denoted with  $T_{lm}^N$  for  $l = 1, \dots, N, m = -l, \dots, l$  and a projection  $p_N : C^\infty(\mathbb{S}^2) \rightarrow \mathfrak{su}(N)$  such that, in the operator norm:

- if  $p_N f - p_N g \rightarrow 0$  then  $f = g$
- $p_N \{f, g\} = N^{3/2} [p_N f, p_N g] + O(1/N)$
- $p_N Y_{lm} = T_{lm}^N$ , for any  $l < N$ .

Using the projections  $p_N$ , we can write the quantized Euler equations as:

$$\begin{aligned} \dot{W} &= [P, W] \\ \Delta_N P &= W, \end{aligned} \tag{2}$$

for  $P, W \in \mathfrak{su}(N)$ , where  $P = p_N \psi$ ,  $W = p_N \omega$  and  $\Delta_N$  is the discrete Laplacian defined in [9]. Equations (2) have been studied in various contexts [1, 14, 15, 18, 19], mainly for their formulation on the 2D flat torus. Their numerical integration has been a classical problem [14, 15], being an example of Lie–Poisson system [7]. The main feature of equations (2) is that they possess an increasing number of conservation laws, proportional to  $N$ . In particular, we have that are conserved in time the total energy  $H(W) = 1/2 \text{Tr}(PW)$ , the Casimirs  $C_k(W) = \text{Tr}(W^k)$ , for  $k = 2, \dots, N$  and the linear momentum  $L = (W_x, W_y, W_z)$ , as defined in [15].

Equations (2) have been extensively numerically studied in [15]. In that work, it has been shown how the conservation of the discrete first integrals is determinant in the characterization of the finite state of the fluid. However, it is not clear the role played by each of those. Moreover, equations (2), together with the conservative numerical scheme employed, seem to show a persistent unsteadiness of the fluid for long time, analogously to what observed in [5].

In order to better understand the long-time behaviour of equations (2), and in particular determine whether a steady state is eventually reached, the idea is to analyse the commutator  $[P, W]$ . As it is shown in the next section, the idea is to split the vorticity in a dynamical passive and a dynamical active part. These two can be determined looking at the part of the vorticity which does and does not commute with the matrix  $P$ .

### 3 Vorticity splitting for the quantized Euler equations

In this section, we present and discuss a new vorticity splitting for the quantized Euler equations. As mentioned above, the idea is to derive a dynamical passive,

denoted by  $W_s$ , and a dynamical active, denoted by  $W_r$ , part for the discrete vorticity  $W$ . The splitting we present is natural in the sense that it does not require any ad hoc choice to define it. What we only need is to introduce the projections onto the stabilizer of the discrete stream function  $P$  and onto its orthogonal complement. Finally, we derive and discuss the dynamical equations for  $W_s$  and  $W_r$ .

Let us consider the quantized Euler equations:

$$\begin{aligned}\dot{W} &= [P, W] \\ \Delta_N P &= W,\end{aligned}$$

for  $P, W \in \mathfrak{su}(N)$ . Let us assume  $P$  to be *generic*, i.e. it has all the eigenvalues distinct. Introducing the Frobenius inner product on  $\mathfrak{su}(N)$ , we can define the decomposition of  $W = W_s + W_r$ , where  $W_s$  is the orthogonal projection of  $W$  onto the stabilizer algebra of  $P$ :

$$\text{stab}_P = \{A \in \mathfrak{su}(N) \text{ s.t. } [A, P] = 0\},$$

and  $W_r$  is its orthogonal complement. We notice that  $\text{stab}_P$  can also be defined as:

$$\text{stab}_P = \{A \in \mathfrak{su}(N) \text{ s.t. } A, P \text{ simultaneously diagonalizable}\}.$$

Hence, more explicitly,  $W_s$  can be construct by finding  $E$  unitary which diagonalizes  $P$ ,  $E^\dagger P E = \Lambda$ , and then defining  $\Pi_s : \mathfrak{su}(N) \rightarrow \text{stab}_P$ , such that:

$$W_s := \Pi_s(W) = E \text{diag}(E^\dagger W E) E^\dagger.$$

Hence, the quantized Euler equations can be written as:

$$\dot{W} = [\Delta_N^{-1}(W_s + W_r), W_r].$$

### 3.1 Dynamics of $W_s$ and $W_r$

Consider a general matrix flow on  $\mathfrak{su}(N)$  of the form

$$\dot{P} = F(P), \tag{3}$$

for  $P \in \mathfrak{su}(N)$  and  $F : \mathfrak{su}(N) \rightarrow \mathfrak{su}(N)$  smooth. Let  $E$  and  $\Lambda$  be an eigenbasis and the corresponding eigenvalues of  $P$ . We want to determine the evolution of  $E$  and  $\Lambda$ . It is known that  $\mathfrak{su}(N)$  is foliated into (co-adjoint) orbits defined as:

$$\mathcal{O}_P = \{Q = U P U^* \text{ for } U \in S U(N)\}.$$

The tangent space at  $P \in \mathfrak{su}(N)$  to the orbit  $\mathcal{O}_P$  is spanned by  $\{e_k e_l^\dagger\}_{k \neq l}$ <sup>1</sup> where  $E = [e_1, \dots, e_N]$  is an orthonormal eigenbasis of  $P$ . If we take the normal directions

---

<sup>1</sup>Here we assume  $P$  generic, i.e., with all the eigenvalues distinct.

$\text{span}\{e_k e_k^\dagger\}$  of the tangent spaces (w.r.t. the canonical bi-invariant inner product), we obtain the linear subspace of matrices in  $\mathfrak{su}(N)$  sharing the same eigenbasis (simultaneously diagonalizable). In the language of Lie algebras, it corresponds to the infinitesimal isotropy algebra corresponding to  $P$ . Thus, if  $\Pi_s: \mathfrak{su}(N) \rightarrow \mathfrak{su}(N)$  denotes orthogonal projection onto  $\text{span}\{e_k e_k^\dagger\}$ , then  $\Pi_r = \text{Id} - \Pi_s$ . Numerically,  $\Pi_s X$  is computed as  $\Pi_s X = E \text{diag}(E^\dagger X E) E^\dagger$ . Notice, as expected, that neither  $\Pi_s$  nor  $\Pi_r$  depend on the eigenvalues of  $P$ , only the eigenbasis. This means that we can write equation (3) as

$$\dot{P} = \Pi_r F(P) + \Pi_s F(P)$$

The first part of the flow,  $\dot{P} = \Pi_r F(P)$ , changes the eigenbasis but not the eigenvalues and vice versa. The question is: what is the generator of  $P \mapsto \Pi_r F(P)$ ? Since it is isospectral it should be of the form  $P \mapsto [B(P), P]$ , but what is  $B(P)$ ? Let us denote  $X = F(P)$ . It is then straightforward to check that if all the eigenvalues  $p_1, \dots, p_N$  of  $P$  are different, then

$$\Pi_r X = \sum_{k \neq l} x_{kl} e_k e_l^\dagger = \sum_{k \neq l} (p_k - p_l) b_{kl} e_k e_l^\dagger = \left[ \sum_{k \neq l} b_{kl} e_k e_l^\dagger, P \right] = [B, P]$$

where  $x_{kl}$  are the components of  $X$  in the basis  $E$ , and  $b_{kl} := x_{kl}/(p_k - p_l)$ . Thus, in the generic case, with all eigenvalues different, we can construct the generator  $B(P)$  from the eigenvalues  $p_1, \dots, p_N$  and the eigenbasis  $e_1, \dots, e_N$  of  $P$ . This allows us to write the equation (3) in terms of the eigenvalues and eigenbasis of  $P$  as

$$\begin{aligned} \dot{p}_k &= e_k^\dagger F e_k, & F &= F \left( \sum_{k=1}^N p_k e_k e_k^\dagger \right) \\ \dot{e}_k &= B e_k, & B &= \sum_{k \neq l} \frac{e_k^\dagger F e_l}{p_k - p_l} e_k e_l^\dagger \end{aligned}$$

**Remark 1.** The evolution of the eigenbasis of  $P$  plays a major role in the variation of the energy metric  $H(P) = 1/2 \text{Tr}(\Delta_N P P)$ . Using that

$$\Delta_N P = [X_0, [X_0, P]] + \frac{1}{2} [X_-, [X_+, P]] + \frac{1}{2} [X_+, [X_-, P]]$$

we see that

$$E^\dagger \Delta_N P E = [Y_0, [Y_0, \Lambda_P]] + \frac{1}{2} [Y_-, [Y_+, \Lambda_P]] + \frac{1}{2} [Y_+, [Y_-, \Lambda_P]]$$

where  $Y_i = E^\dagger X_i E$ , i.e., the matrices  $X_i$  expressed in the eigenbasis  $E$ . Thus, the  $Y_i$  are also transported by the generator  $B$ , so they can be thought of as advected quantities

$$\dot{Y}_i = \pm [B, Y_i].$$

Deforming  $Y_i$  somehow corresponds to deforming the metric via a symplectomorphism. Notice, however, that the  $Y_i$  are complicated from the start (since  $E$  is complicated from the start).

**Remark 2.** The matrices  $E_{kk} = ie_k e_k^\dagger$ , for  $k = 1, \dots, N$  form an orthonormal basis for  $\text{stab}_P$ . In particular, these elements can have an interpretation as moving frame, which varies accordingly to the evolution of  $P$ . Furthermore, by plotting them, it is remarkable that they correspond to some kind of wavelet basis. Indeed, for the Euler equations, the interpretation of the spectral decomposition of  $P$  is such that its eigenvalues correspond to the values that the respective stream function takes, whereas its eigenvectors (or the matrices  $E_{kk}$ ) correspond to the connected components of the level curves of the respective stream function (see Figure 1).

Let us now consider the matrix flow for  $W_s$  and  $W_r$ . By the definition of  $W_s$  we have that:

$$\begin{aligned}\dot{W}_s &= \frac{d}{dt} \left( E \text{diag}(E^\dagger W E) E^\dagger \right) \\ &= [E E^\dagger, W_s] - \Pi_s([\dot{E} E^\dagger, W_r]),\end{aligned}$$

where we have used the fact that  $\Pi_s(\dot{W}) = 0$  and  $\dot{E} E^\dagger = -E \dot{E}^\dagger$ . This dynamics is very close to the one of  $P$ :

$$\dot{P} = [\dot{E} E^\dagger, P] + E \dot{D}_P E^\dagger.$$

Hence, it is crucial to determine a formula for  $\dot{E} E^\dagger$ . To this end, we know that the dynamics of  $P$  can be orthogonally decomposed as:

$$\dot{P} = \Pi_r(\Delta_N^{-1}[P, \Delta P]) + \Pi_s(\Delta_N^{-1}[P, \Delta P]).$$

Hence, it is clear that:

$$[\dot{E} E^\dagger, P] = \Pi_r(\Delta_N^{-1}[P, \Delta P]).$$

We notice that  $\dot{E} E^\dagger$  can be taken in  $\text{stab}_P^\perp$ . In fact, the dynamics of  $W_s$  remains the same for any  $\dot{E} E^\dagger + S$ , where  $S \in \text{stab}_P$ . The map:

$$[\cdot, P] : \text{stab}_P^\perp \rightarrow \text{stab}_P^\perp$$

is invertible and  $\dot{E} E^\dagger$  is uniquely determined in  $\text{stab}_P^\perp$ . Hence, in conclusion we have the following theorem for the dynamics of  $W_s, W_r$ :

**Theorem 1.** *Let  $W$  be a solution to equations (2) and  $W_s, W_r$  respectively be the orthogonal projections of  $W$  onto  $\text{stab}_P$  and its orthogonal complement. Then,  $W_s$  and  $W_r$  satisfy the following system of equations:*

$$\begin{aligned}\dot{W}_s &= [B, W_s] - \Pi_s[B, W_r] \\ \dot{W}_r &= -[B, W_s] + \Pi_s[B, W_r] + [P, W_r] \\ [B, P] &= \Pi_r \Delta_N^{-1}[P, W_r],\end{aligned}$$

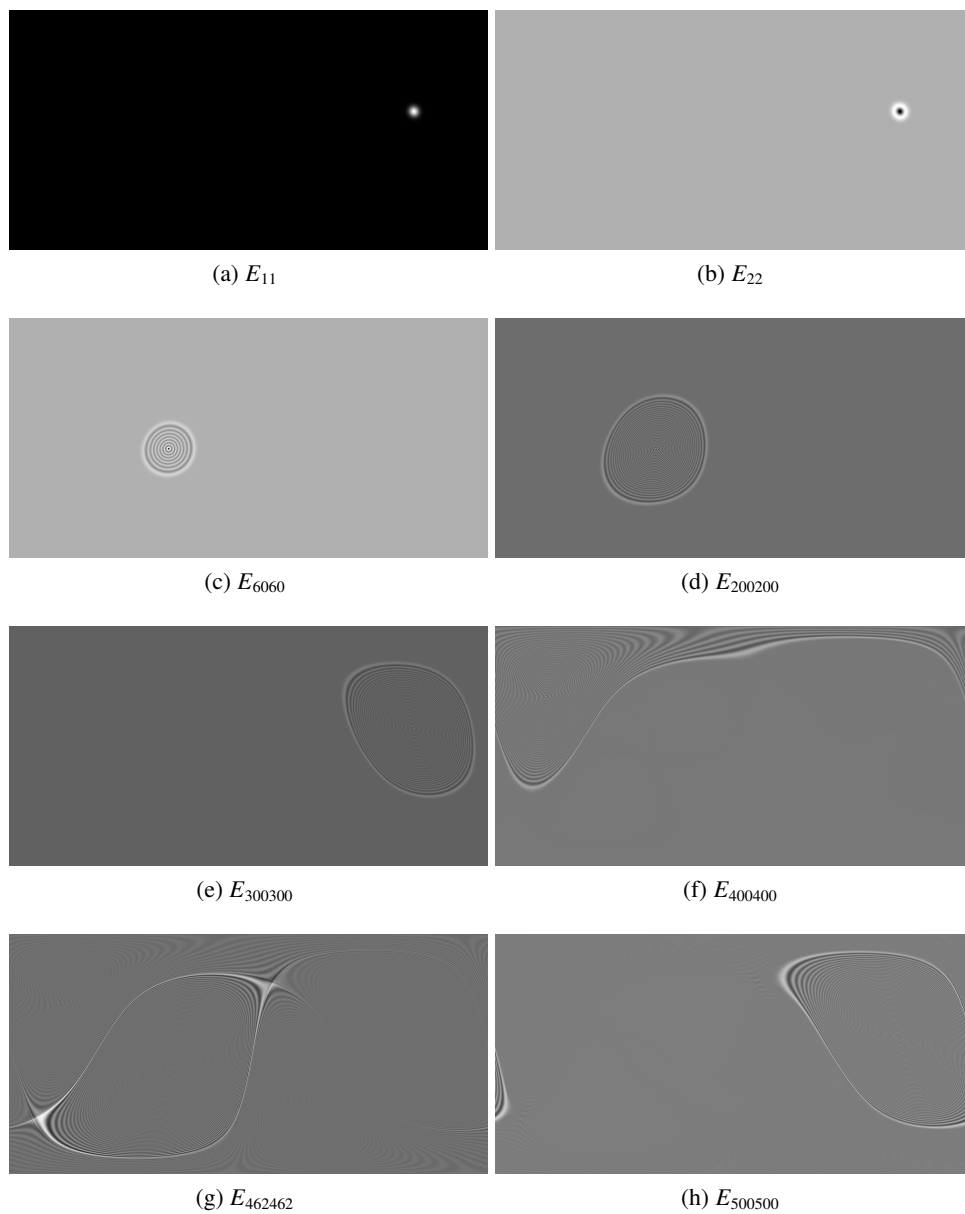


Figure 1: Some basis element of  $\text{stab}_P$  at  $t = t_{\text{end}}$  for the first numerical simulation of Section 4.



where  $B$  is the unique solution to the third equation in  $\text{stab}_P^\perp$  and  $P = \Delta_N^{-1}(W_s + W_r)$ .

From theorem 1, we can deduce some facts about the  $W_s, W_r$  dynamics. First of all, we notice that if  $W_r = 0$  then  $B = 0$ . In fact, if  $W_r = 0$ , we get that  $B \in \text{stab}_P \cap \text{stab}_P^\perp$ . Hence  $B = 0$ . Conversely, if  $B = 0$ , we get that  $\dot{W}_s = 0$  and  $\dot{W}_r = [P, W_r]$ . Hence, in that case  $W_s$  plays the role of a fixed topography for  $W_r$ , which satisfies a Euler-type equation. From the third equation, we deduce that it must be

$$\text{Tr}(\Delta_N^{-1} W_s [\Delta_N^{-1} W_r, W_r]) = 0. \quad (4)$$

Equation (4) and  $B = 0$  imply that the energy  $H(W_r)$  is conserved and provides a full separation of scales, for which the large scales are in equilibrium, whereas the small scales have still some dynamics left, which does not affect the large ones.

An other observation is that if  $[B, W_s] = 0$ , then  $B = 0$  and so  $\dot{W}_s = 0$ . Vice versa, if  $\Pi_s[B, W_r] = 0$ , then again we deduce that  $\text{Tr}(\Delta_N^{-1} W_s [\Delta_N^{-1} W_r, W_r]) = 0$ . These facts can be interpreted saying that it is possible to have an evolution of the eigenvectors of  $P$  without any change of the eigenvalues, but not vice versa.

### 3.2 Energy and enstrophy splitting

Let us now look in how the energy and the enstrophy are related to the splitting  $W_s$  and  $W_r$ . By definition, the energy  $H$  can be written as:

$$\begin{aligned} H(W) &= \frac{1}{2} \text{Tr}(\Delta_N^{-1} (W_s + W_r) W_s) \\ &= \frac{1}{2} \text{Tr}(\Delta_N^{-1} (W_s) W_s) - \frac{1}{2} \text{Tr}(\Delta_N^{-1} (W_r) W_r) \end{aligned}$$

and the enstrophy

$$E(W) = -\text{Tr}(W_s^2) - \text{Tr}(W_r^2).$$

Hence, we have the interesting fact that

$$\begin{aligned} H(W) &= H(W_s) - H(W_r) \\ E(W) &= E(W_s) + E(W_r). \end{aligned} \quad (5)$$

We notice that  $W_s = 0$  if and only  $W = 0$ , being  $\sqrt{H(\cdot)}$  a norm. Moreover, if  $W \neq 0$ ,

$$0 < H(W) \leq H(W_s) < E(W_s) \leq E(W).$$

The fact that the energy of  $W_s$  is larger than the total energy  $H(W)$  can be interpreted as the fact that the large scales  $W_s$  are slowed down by the small scales  $W_r$ , which acts as a dissipative field, moving the energy towards the small scales (see figure 4).

It is possible to represent the energy-ensrophy splitting (5) in a more geometric way. The first equation of (5) tells that  $W$  and  $W_r$  are orthogonal in the energy norm, whereas the second equation says that  $W_s$  and  $W_r$  are orthogonal in the  $L^2$  norm. Let us take the  $W, W_r$ -plane, and let  $r := \sqrt{H(W_r)}$  and  $H_0 = \sqrt{H(W)}$ . Then, for  $W_r = (0, r)$  and  $W = (H_0, 0)$ , the energy norm is the identity matrix on  $\mathbb{R}^2$ . We want to express the  $L^2$  norm with respect the energy norm. Let us first observe that  $W_s = (H_0, -r)$ . Then, the  $L^2$  norm can be defined as  $G = C^*C$ , where  $C : \mathbb{R}^2 \rightarrow \mathbb{R}^2$  is such that  $C(0, r)^T = (0, E_0 \sin \alpha)^T$  and  $C(H_0, 0)^T = E_0(\cos \alpha, \sin \alpha)^T$ , where  $\alpha$  is the angle between  $W$  and  $W_s$  in the  $L^2$  norm and  $E_0 = \sqrt{E(W)}$ . Then, we have that:

$$G = \begin{bmatrix} \frac{E_0^2}{H_0^2} & \frac{E_0^2}{rH_0} \sin^2 \alpha \\ \frac{E_0^2}{rH_0} \sin^2 \alpha & \frac{E_0^2}{r^2} \sin^2 \alpha \end{bmatrix},$$

in the  $W, W_r$ -plane. We can derive the following inequalities:

$$\begin{aligned} r &= \sqrt{H(W_r)} \leq \sqrt{E(W_r)} = E_0 |\sin \alpha| \\ N^2 r &= N^2 \sqrt{H(W_r)} \geq \sqrt{E(W_r)} = E_0 |\sin \alpha|. \end{aligned}$$

Hence, if  $\sin \alpha \neq 0$ , we get that:

$$\frac{E_0}{N^2} \leq \frac{r}{|\sin \alpha|} \leq E_0. \quad (6)$$

Therefore, we see that in the limit for  $N \rightarrow \infty$  the ratio  $\frac{|\sin \alpha|}{r}$  is potentially unbounded. Indeed, it could happen that the  $L^2$  norm of  $W_r$  is always far from being zero, whereas its energy norm goes to zero. This corresponds to the case when  $W_r$  is shifted more and more towards the small frequencies keeping its enstrophy large. Because of the inequality (6), we notice that in the finite dimensional case this can never occur.

## 4 Some heuristic considerations on the vorticity splitting

In this section, we want to present some results concerning the splitting of  $W_s$  and  $W_r$ . Our observations are based on some numerical evidences and heuristic considerations. One main motivation for studying the vorticity splitting in the  $W_s$  and  $W_r$  component is that the unsteadiness of the fluid can be precisely understood in terms of non-vanishing of  $W_r$ . Moreover, in order to derive  $W_s$  and  $W_r$ , it is not required any knowledge of neither the Fourier decomposition nor the values of  $W$ . From an analytical point of view,  $W_s$  represents a projection of  $W$  onto a smoother

subspace. Indeed, the relation via the Laplace operator between  $P$  and  $W$  says that  $P$  admits, in general, two more spatial derivatives than  $W$ . Hence, since  $W_s$  is related to  $P$  via a polynomial relationship,  $W_s$  is in general more regular than  $W$ . Vice versa,  $W_r$  contains the rougher part of  $W$ . The tempting interpretation of the vorticity splitting above presented is that  $W_s$  represents the low dimensional large scale dynamics, whereas  $W_r$  represents the noisy small scale dynamics.

In order to assess this conjecture, we consider the numerical simulation studied in [5, 15]. In Figure 2 the three vorticity fields  $W, W_s, W_r$  are shown at the times  $t = t_0$  and  $t = t_{end} \sim 10^2 s$ . As expected, at the end of the simulation, the large scales of the vorticity are all contained in the smooth field  $W_s$ , whereas  $W_r$  is almost everywhere white noise. In Figure 3, we have plotted the field  $B$  at  $t = t_{end}$  and the relation between the values taken by  $P$  and  $W_s$ , in their spatial plot. It is quite clear that far from the center of the blobs the level curves of  $B$  and  $W_s$  are very close one to the other, even though they do not commute. A possible interpretation of this fact is that the most of the dynamics is concentrated around the blobs, where the mixing of the vorticity continues for very long (infinite) time. Furthermore, we notice that  $B$  has exactly two saddle points and those correspond to the bifurcations appearing in the  $P - W_s$  plot. The branches in the  $P - W_s$  plot correspond to the fact that four main blobs emerge. Clearly, the fact that the plot is not a graph of a function implies that a possible functional relation between  $W_s$  and  $P$  can only be local in space.

The scale separation of the vorticity is even more clear looking at the energy spectrum of  $W$ . In Figure 4, we have plotted in log-log scale the energy diagrams of the three vorticity fields  $W, W_s, W_r$  at  $t = t_{end}$ . The energy level  $H(l)$ , corresponding to the wave-number  $l = 1, \dots, N$ , encodes the energy of the modes with respect to the harmonics  $Y_{lm}$ , for  $m = -l, \dots, l$ . We notice that the energy spectrum of  $W$  is analogous to the one obtain in [2]. We can see that the two slopes in the energy spectrum of  $W$  depend on the fact that the first  $l^{-3}$  slope comes from the energy spectrum of  $W_s$ , whereas the  $l^{-1}$  slope comes from the energy spectrum of  $W_r$ . In this sense, we can say that the vorticity splitting is a scale separation of the vorticity field.

We consider another numerical simulation, where the three blob formation emerges, as predicted in [15]. In Figure 5 the three vorticity fields  $W, W_s, W_r$  are shown at the times  $t = t_0$  and  $t = t_{end} \sim 10^2 s$ . As expected, at the end of the simulation, the large scales of the vorticity are all contained in the smooth field  $W_s$ , whereas  $W_r$  is almost everywhere white noise. In Figure 6, we have plotted the field  $B$  at  $t = t_{end}$  and the relation between the values taken by  $P$  and  $W_s$ , in their spatial plot. In contrast with the one of Figure 3, we notice that there is only one saddle point, which corresponds to the bifurcation appearing in the  $P - W_s$  plot. The branches in the  $P - W_s$  plot correspond to the fact that three main blobs

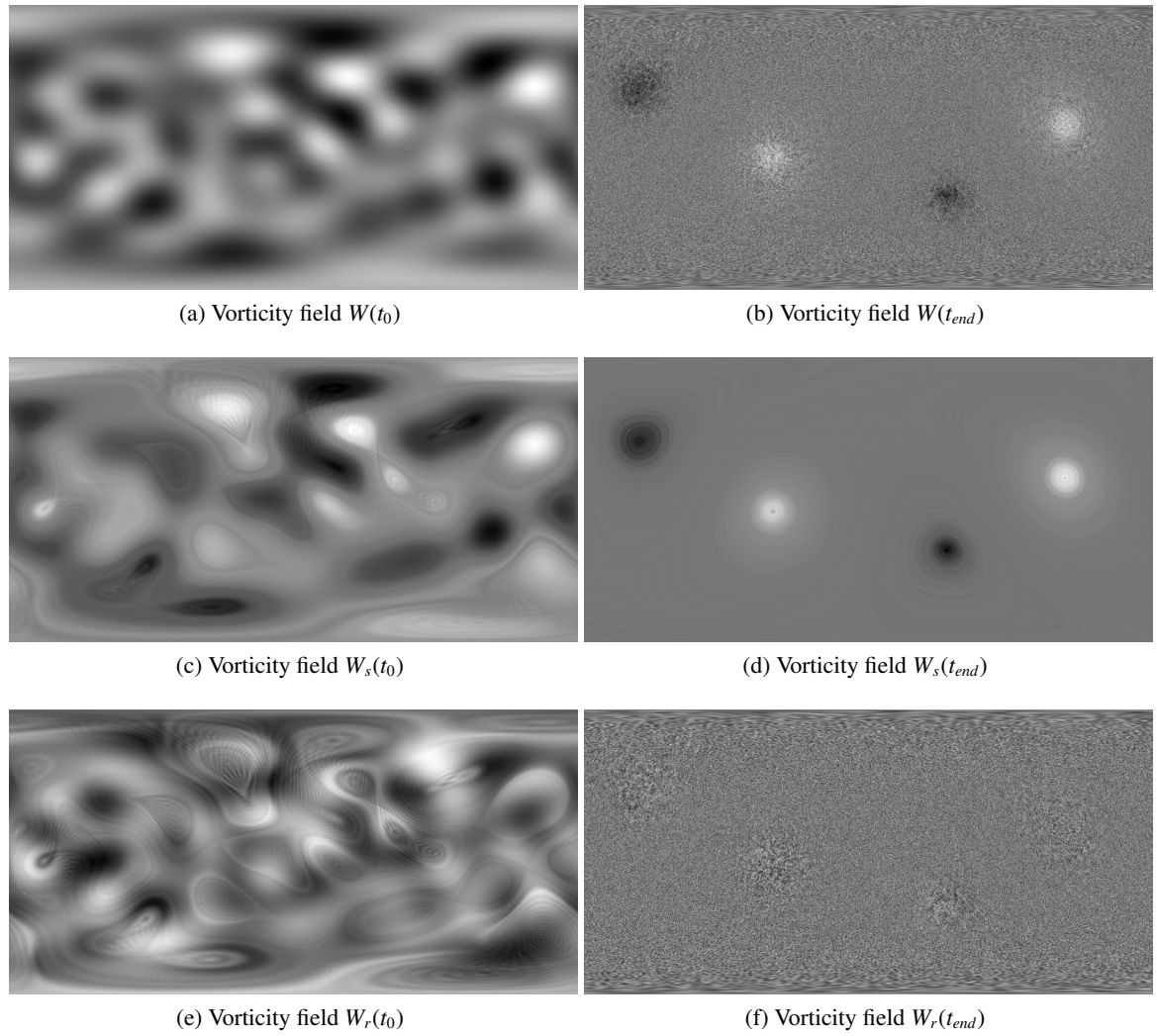
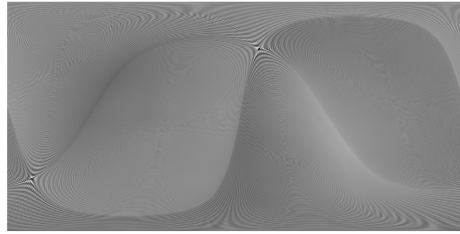
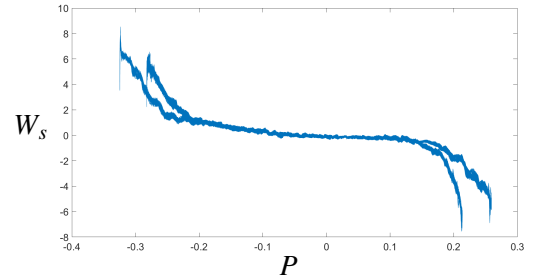


Figure 2: The three vorticity fields  $W$ ,  $W_s$ ,  $W_r$  at  $t = t_0$  and  $t = t_{end}$ .



(a)  $B$  field at  $t = t_{end}$



(b)  $P - W_s$  values at  $t = t_{end}$

Figure 3

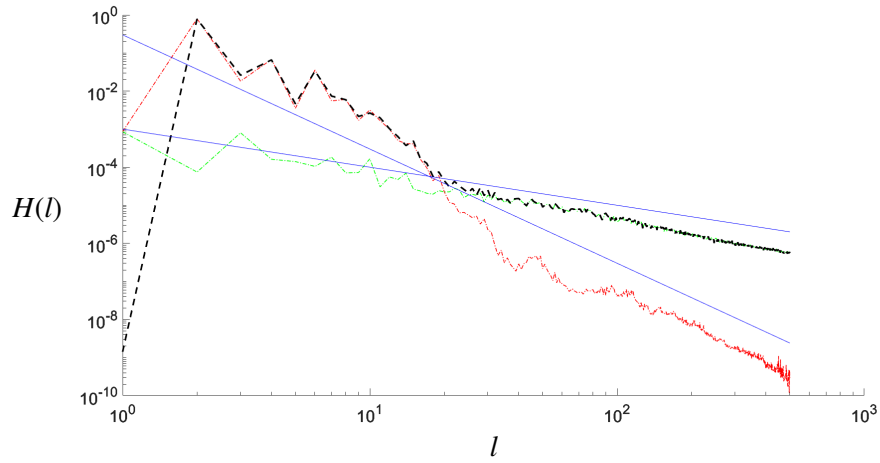
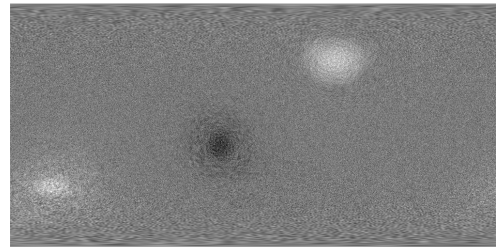


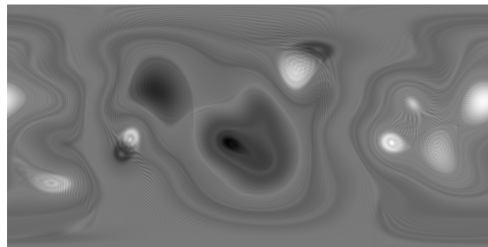
Figure 4: Energy spectrum in log-log scale of the three vorticity fields  $W$  dashed black,  $W_s$  dashed-dot red,  $W_r$  dashed-dot green at  $t = t_0$  and  $t = t_{end}$ . In blue are reported the slopes  $l^{-3}$  and  $l^{-1}$ .



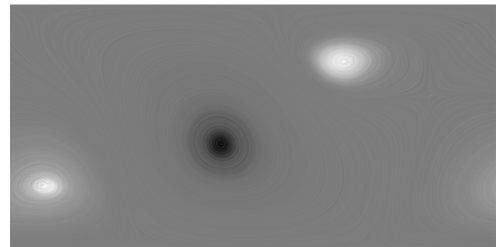
(a) Vorticity field  $W(t_0)$



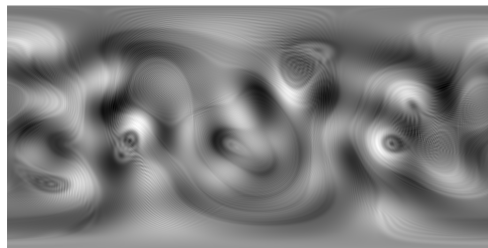
(b) Vorticity field  $W(t_{end})$



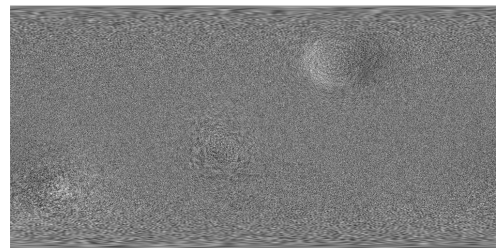
(c) Vorticity field  $W_s(t_0)$



(d) Vorticity field  $W_s(t_{end})$

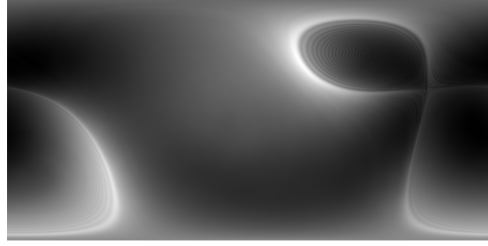


(e) Vorticity field  $W_r(t_0)$

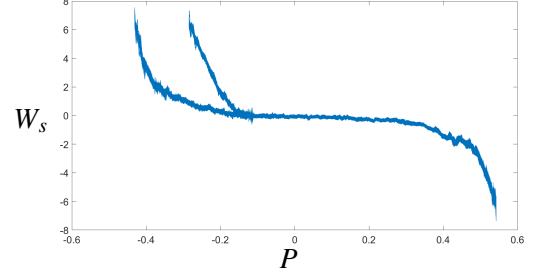


(f) Vorticity field  $W_r(t_{end})$

Figure 5: The three vorticity fields  $W$ ,  $W_s$ ,  $W_r$  at  $t = t_0$  and  $t = t_{end}$ .



(a)  $B$  field at  $t = t_{end}$



(b)  $P - W_s$  values at  $t = t_{end}$

Figure 6

emerge. Hence, looking at Figure 3-6, we see a clear connection between saddle points of  $B$  and the number of blobs.

The scale separation of the vorticity is again evident looking at the energy spectrum of  $W$ . In Figure 4, we have plotted in log-log scale the energy diagrams of the three vorticity fields  $W, W_s, W_r$  at  $t = t_{end}$ . We notice that the energy spectrum of  $W$  is analogous to the one in Figure 4.

Finally, we remark that the projection  $\Pi_s : \mathfrak{su}(N) \rightarrow \text{stab}_P$  has rank  $N$ . Hence, the dynamics of  $W_s$  in the moving frame  $E_{kk}$  can be described by only  $N$  components, i.e. its eigenvalues. Therefore, the vorticity splitting can be also interpreted as a reduced dynamics.

## 5 Vorticity splitting in the continuous case

In this section we consider the Euler equations for the vorticity:

$$\begin{aligned} \dot{\omega} &= \{\psi, \omega\} \\ \Delta\psi &= \omega. \end{aligned} \tag{7}$$

where  $\omega \in C^1([0, \infty), C^k(\mathbb{S}^2))$ , for some  $k \geq 1$ . In order to define the analogous of the finite dimensional splitting, we have to understand equations (7) in the weak sense. Indeed, we will show that in general the analogous of the projections  $\Pi_s, \Pi_r$  cannot preserve the smoothness of  $\omega$ . However, they are still continuous with operator norm one, from  $C^k(\mathbb{S}^2)$  to  $L^p(\mathbb{S}^2)$ , for any  $k \in [0, \infty], p \in [1, \infty]$ . Hence, by density of the smooth functions in  $L^p(\mathbb{S}^2)$ ,  $p \in [1, \infty)$  we can extend  $\Pi_s, \Pi_r$  to continuous operator to  $L^\infty(\mathbb{S}^2)$ . This result fits very well with the well-posedness of equations (7), which for finite domains precisely requires a vorticity in  $L^\infty$ , [13, Chp. 2.3].

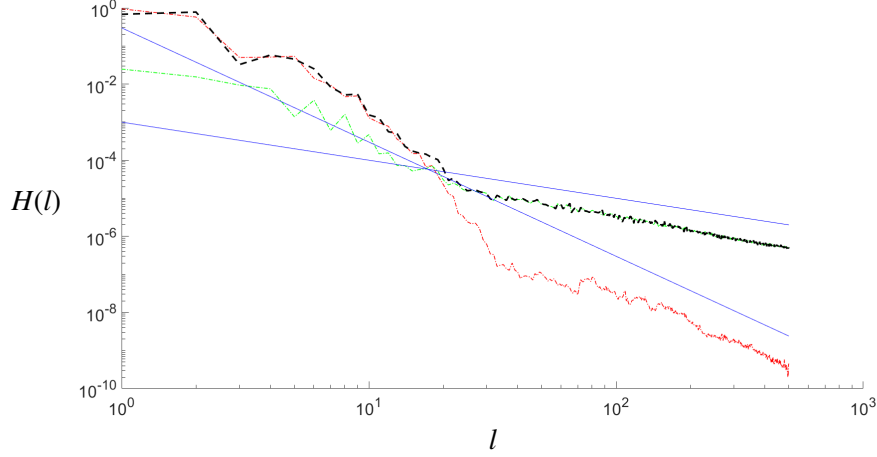


Figure 7: Energy spectrum in log-log scale of the three vorticity fields  $W$  dashed black,  $W_s$  dashed-dot red,  $W_r$  dashed-dot green at  $t = t_0$  and  $t = t_{end}$ . In blue are reported the slopes  $l^{-3}$  and  $l^{-1}$ .

Let us first define the right hand side of equations (7) in the weak sense. For any  $p \geq 2$ , let  $\omega \in L^p(\mathbb{S}^2)$ . Then,  $\psi \in W^{2,p}(\mathbb{S}^2) \subset C^1(\mathbb{S}^2)$ . Finally, we define the weak Poisson bracket as:

$$\int_{\mathbb{S}^2} \{\psi, \omega\} \phi dS = - \int_{\mathbb{S}^2} \omega \{\psi, \phi\} dS,$$

for any test function  $\phi \in C^\infty(\mathbb{S}^2)$ . We can now define the stabilizer of  $\psi$  as:

$$\text{stab}_\psi := \{f \in L^2(\mathbb{S}^2) \text{ s.t. } \{f, \psi\} = 0\}.$$

We want now define the projection  $\Pi_s$  onto  $\text{stab}_\psi$ . One issue is that the stabilizer of  $\psi$  is not closed in  $L^2$  strong topology. However, for continuous functions it is possible to define a projector, which minimizes the  $L^2$  distance from  $\text{stab}_\psi$ . We first take the following assumption on the critical points of  $\psi$

**Assumption 1.** Let  $\psi \in C^1(\mathbb{S}^2)$  be the stream function. Then, the critical points of  $\psi$  define a set of zero Lebesgue measure on  $\mathbb{S}^2$ , such that it is never dense in any neighbourhood of one of its points.

We say that  $\psi$  is *generic*, whenever it satisfies Assumption 1. Let us now consider some  $f \in C^1(\mathbb{S}^2)$ . We see from this definition that  $f \in \text{stab}_\psi$  if and only  $\nabla f$  and  $\nabla \psi$  are parallel. Since we are taking  $\psi$  generic, the points where  $\nabla \psi = 0$  lie



on a set of zero measure, nowhere dense. Therefore, being  $f$  continuous,  $f \in \text{stab}_\psi$  if it is constant on the connected components of the level curves of  $\psi$ . Then the projection of  $f$  onto  $\text{stab}_\psi$  can be defined evaluating  $f$  on the level curves of  $\psi$ , i.e. the streamlines. Let  $\gamma$  be a connected component of a streamline, then we define the projector  $\Pi_s : C^1(\mathbb{S}^2) \rightarrow \text{stab}_\psi$  as:

$$\Pi_s(f)|_\gamma = \frac{1}{\text{length}(\gamma)} \int_\gamma f ds. \quad (8)$$

In the limit case, when  $\gamma$  is a point, clearly  $\Pi_s(\omega)|_\gamma = f(\gamma)$ . We notice that the operator  $\Pi_s$  does not preserve in general the continuity of  $f$ . Indeed, let us call a point  $p \in \mathbb{S}^2$  a *bifurcation saddle point* if  $p$  is a saddle point of  $\psi$  such that the streamline passing through  $p$  contains a bifurcation point. We then have the following result:

**Proposition 1.** *Let  $\psi$  be generic and  $\Pi_s$  the projector as defined in (8). Then, if  $p \in \mathbb{S}^2$  is a bifurcation saddle point for  $\psi$ , there exists  $f \in C^1(\mathbb{S}^2)$ , such that  $\Pi_s(f)$  is discontinuous at the streamline passing through  $p$ . Viceversa, given  $f \in C^1(\mathbb{S}^2)$ , if  $\Pi_s(f)$  is discontinuous at some point  $p \in \mathbb{S}^2$ , then the streamline passing through  $p$  contains a bifurcation saddle point.*

*Proof.* [Sketch] The issue about the continuity of  $f$  can be treated locally. Hence, let us work in Cartesian coordinates  $x, y$ . Let  $p \in \mathbb{S}^2$  be a bifurcation saddle point for  $\psi$  and  $\gamma$  the streamline passing through  $p$ . Then, let  $\beta$  be a curve intersecting  $\gamma$  only in  $p$  and let  $f$  be a smooth function positive at one side of  $\beta$  and negative at the other one, such that  $\int_\gamma f ds = 0$ . Then being  $p$  a bifurcation point, for any neighbourhood  $U$  of  $p$ , there exist streamlines totally contained in one or another side of  $\beta$ . Then, the average of  $f$  on those streamlines is either strictly positive or negative, creating a discontinuity at  $\gamma$ .

Viceversa, let  $f \in C^1(\mathbb{S}^2)$ , such that  $\Pi_s(f)$  is discontinuous at some point  $p \in \mathbb{S}^2$ . Then, the streamline passing through  $p$  cannot be homomorphic to any of those in some tubular neighbourhood. Hence, the streamline passing through  $p$  must contain a critical point for  $\psi$ , which also is a bifurcation saddle point.  $\square$

However, we have the following regularity for  $\Pi_s$ . The operator  $\Pi_s$  is a bounded operator with unitary norm between  $C^1(\mathbb{S}^2)$  and  $L^p(\mathbb{S}^2)$ , for every  $p \in [1, \infty]$ . Since  $C^1(\mathbb{S}^2)$  is dense in any  $L^p(\mathbb{S}^2)$ , for  $p \in [1, \infty)$ , it is possible to extend  $\Pi_s$  to any  $L^p(\mathbb{S}^2)$ , for every  $p \in [1, \infty)$ . By the continuity of the  $L^p$  norm with respect to  $p$ , we conclude that we can also extend  $\Pi_s$  to a bounded operator on  $L^\infty(\mathbb{S}^2)$ .

Hence, from now on, let us consider equations (7) in the weak form, for  $\omega \in L^\infty(\mathbb{S}^2)$ . It is clear that  $\Pi_s^2 = \Pi_s$ . Moreover, we can formally define the operator

$\Pi_s$  via the kernel  $K(x, y) = \frac{1}{\text{length}(\gamma_x)} \delta_{\gamma_x}(y)$ , for any  $x, y \in \mathbb{S}^2$ , where  $\gamma_x$  is the connected component of the streamline passing in  $x$ . In this way we get that  $\Pi_s$  is self-adjoint with respect to the  $L^2$  inner product:

$$\begin{aligned} \int_{\mathbb{S}^2} f \Pi_s g dS &= \int_{\mathbb{S}^2} f(x) \int_{\mathbb{S}^2} K(x, y) g(y) dS(y) dS(x) \\ &= \int_{\mathbb{S}^2} g(y) \int_{\mathbb{S}^2} K(x, y) f(x) dS(x) dS(y) \\ &= \int_{\mathbb{S}^2} g \Pi_s f dS, \end{aligned}$$

for any  $f, g \in C^1(\mathbb{S}^2)$ . Then, by extension we get the same result in  $L^\infty(\mathbb{S}^2)$ .

Then, we have the following proposition:

**Proposition 2.** *Let  $f \in L^\infty(\mathbb{S}^2)$  and  $\psi$  be generic. Then  $f \in \text{stab}_\psi$  if and only if  $\Pi_s f = f$ .*

*Proof.* Let us prove the result for  $f \in C^1(\mathbb{S}^2)$ , and conclude by extension. Let  $f \in \text{stab}_\psi$ . Then,  $\nabla f$  is parallel to  $\nabla \psi$  almost everywhere. Hence, the gradient of  $f$  along any streamline must vanish, and so on each connected component it is constant. By continuity of  $f$  we deduce that  $f$  must be constant also on the streamlines containing some critical points. Therefore,  $\Pi_s(f) = f$ .

Let us now assume that  $\Pi_s(f) = f$ . Then,  $f$  must be constant on each connected component of a streamline. Hence,  $\nabla f$  is orthogonal to the streamlines. Since,  $\nabla \psi$  is also orthogonal to the streamlines, we conclude that  $\{f, \psi\} = 0$  and so  $f$  is in  $\text{stab}_\psi$ .  $\square$

Hence, we can derive the analogous results of Section 3 for the continuous case. First of all, let us recall that the stream function  $\psi$  satisfies the equation:

$$\dot{\psi} = \Delta^{-1}\{\psi, \Delta\psi\}. \quad (9)$$

Equation (9) is not Hamiltonian, but we can split the right hand side into the Hamiltonian and non-Hamiltonian part, using the projection  $\Pi_s$ :

$$\dot{\psi} = \Pi_r \Delta^{-1}\{\psi, \Delta\psi\} + \Pi_s \Delta^{-1}\{\psi, \Delta\psi\}.$$

Analogously to the finite dimensional case, we would like to find a generator for part  $\Pi_r \Delta^{-1}\{\psi, \Delta\psi\}$ . In particular, we would like to find a function  $b$ , such that

$$\{b, \psi\} = \Pi_r \Delta^{-1}\{\psi, \Delta\psi\}. \quad (10)$$

It is clear that a necessary condition for the equation  $\{b, \psi\} = f$  to have a solution  $b$ , is that  $f \in \text{stab}_\psi^\perp$ . Indeed, we have that for any  $b \in C^1(\mathbb{S}^2)$ ,  $\{b, \psi\} \in \text{stab}_\psi^\perp$ , as it is easily checked:

$$\int_{\mathbb{S}^2} \{b, \psi\} g dS = - \int_{\mathbb{S}^2} \{g, \psi\} b dS = 0,$$

for any  $g \in \text{stab}_\psi$ . However, in general equation (10) can be solved only where  $\nabla\psi \neq 0$ . Around the critical points of  $\psi$  the gradient of  $b$  is potentially unbounded. Moreover, the right hand side in equation (10) can be discontinuous at the level curves of  $\psi$  containing saddle points of  $\psi$ . Hence,  $b$  can only be defined almost everywhere. Furthermore, we have the following:

**Proposition 3.** *Let  $f \in C^0(\mathbb{S}^2)$  and  $\psi$  generic. Then,  $f \in \text{stab}_\psi^\perp$  if and only if there exists  $b$  almost everywhere smooth, such that  $\{b, \psi\} = f$ , where  $\nabla\psi \neq 0$ .*

*Proof.* The if part is clear. Let instead take  $f \in \text{stab}_\psi^\perp$ . Then, for any point  $p \in \mathbb{S}^2$ , we have to solve the PDE for  $b$ :

$$\nabla\psi^\perp \cdot \nabla b = f, \quad (11)$$

where  $\nabla\psi^\perp = p \times \nabla\psi$ . If  $\nabla\psi$  does not vanish, equation (11) can be solved by integration in the direction of  $\nabla\psi^\perp$ . In the points where  $\nabla\psi$  does not vanishes,  $\nabla b$  is not defined by equation (11), and it can be unbounded around those points. Hence, the field  $b$  is almost everywhere smooth and satisfies  $\{b, \psi\} = f$ , where  $\nabla\psi \neq 0$ .  $\square$

In order to derive the dynamical equations for  $\omega_s$ , we cannot use directly the field  $b$ . Instead, we consider the volume preserving vector field

$$X[\psi] := \Pi_r \Delta^{-1} \{\psi, \Delta\psi\}.$$

We note that  $X$  corresponds to the infinitesimal action of a map  $\varphi_t$  which transports  $\psi$  by deforming its level curves. Hence,  $\varphi_t$  extends naturally to action on  $\text{stab}_\psi$ . Let us write  $\Pi'_s$  the projection onto  $\text{stab}_\psi$  at time  $t$ . Then, for any point  $x \in \mathbb{S}^2$ , let  $\gamma(t) = \{y | \psi(y) = \psi(x) \text{ and } y \text{ belongs to the same connected component of } \mathbf{x}\}$ , and  $d\hat{s}_t$  the normalized Lebsgue measure on  $\gamma(t)$ . We have then the formal identity:

$$\begin{aligned} \omega_s(t, x) &= \Pi'_s \omega(t, x) \\ &= \int_{\gamma(t)} \omega(t, y) d\hat{s}_t(y) \\ &= \int_{\gamma(0)} (\varphi_t^* \omega)(t, y) d\hat{s}_0(y) \\ &= \Pi_s^0 (\varphi_t^* \omega)(t, \varphi_t^{-1}(x)). \end{aligned}$$

Hence, for any test function  $\phi \in C^\infty(\mathbb{S}^2)$ , we have

$$\begin{aligned} \frac{d}{dt} \int_{\mathbb{S}^2} \omega_s(t, x) \phi(x) dS &= \frac{d}{dt} \int_{\mathbb{S}^2} \Pi_s^0(\varphi_t^* \omega)(t, \varphi_t^{-1}(x)) \phi(x) dS \\ &= \int_{\mathbb{S}^2} \left( \Pi_s^0(\varphi_t^* \mathcal{L}_X \omega)(t, \varphi_t^{-1} x) - \mathcal{L}_X \Pi_s^0(\varphi_t^* \omega)(t, \varphi_t^{-1} x) \right) \phi(x) dS \\ &= - \int_{\mathbb{S}^2} \omega(t, x) \mathcal{L}_X \Pi_s^t \phi(x) + \mathcal{L}_X \Pi_s^t \omega(t, x) \phi(x) dS \end{aligned}$$

where  $\mathcal{L}_X$  is the Lie derivative, which simply acts on functions as  $\mathcal{L}_X f = X[f]$ . We notice from the previous calculations that  $\mathcal{L}_X$  has to be evaluated only on elements in  $\text{stab}_\psi$ . Hence, the time derivative of  $\omega_s$  is well defined in the weak sense.

Let us now formally denote  $X := -\{b, \cdot\}$ . Then, interpreting the Poisson bracket in the weak sense, we can write the dynamical system for  $\omega_s, \omega_r$  as:

$$\begin{aligned} \dot{\omega}_s &= \{b, \omega_s\} - \Pi_s \{b, \omega_r\} \\ \dot{\omega}_r &= -\{b, \omega_s\} + \Pi_s \{b, \omega_r\} + \{\psi, \omega_r\} \\ \{b, \psi\} &= \Pi_r \Delta^{-1} \{\psi, \omega_r\}, \end{aligned}$$

where  $b$  is implicitly defined by the third equation and  $\psi = \Delta^{-1}(\omega_s + \omega_r)$ . We notice that the equations of motion for  $\omega_s$  can also be written in a more compact form as:

$$\dot{\omega}_s = [\Pi_s, \mathcal{L}_X] \omega,$$

where the square bracket is a commutator of operators.

Finally, we notice that the energy and enstrophy splitting still hold:

$$\begin{aligned} H(\omega) &= H(\omega_s) - H(\omega_r) \\ E(\omega) &= E(\omega_s) + E(\omega_r). \end{aligned}$$

## Appendix A: Stream function splitting

In this section, we present the analogous splitting of Section 3 for the stream function  $P$ . Let  $\text{stab}_W$  be the stabilizer of  $W$  in  $\mathfrak{su}(N)$ . Then, we can consider the stream function splitting  $P = P_s + P_r$ , where  $P_s$  is the orthogonal projection of  $P$  onto  $\text{stab}_W$ , and  $P_r$  the orthogonal complement. Similarly to what we have done in Section 3,  $P_s$  can be constructed by finding  $U$  unitary which diagonalizes  $W$ :

$$U^* W U = D,$$

and then defining  $P_s = U \text{diag}(U^* W U) U^*$ . By definition the quantized Euler equations for the stream function  $P$  can be written as:

$$\dot{P} = \Delta_N^{-1} [P_r, \Delta(P_s + P_r)],$$

the energy  $H(P) = \frac{1}{2}\text{Tr}(\Delta_N(P_s + P_r)P_s) = \frac{1}{2}\text{Tr}(\Delta_N(P_s)P_s) - \frac{1}{2}\text{Tr}(\Delta_N(P_r)P_r)$  and the enstrophy  $E(P) = -\text{Tr}((\Delta_N(P_s + P_r))^2)$ . Notice that the enstrophy  $E(P) = -\text{Tr}((\Delta_N P)^2)$ , in the  $P_s, P_r$  does not admit a splitting contrary to the energy  $H(P) = \text{Tr}(\Delta_N P P)$ :

$$\begin{aligned} H(P) &= H(P_s) - H(P_r) \\ E(P) &\neq E(P_s) + E(P_r). \end{aligned}$$

Since the eigenvalues of  $W$  are constant in time, the dynamics of  $P_s, P_r$  variables is simpler than the one of  $W_s, W_r$ . In fact, we have that  $\dot{U}U = P$  and so

$$\begin{aligned} \dot{P}_s &= [\dot{U}U, P_s] - \Pi_s[\dot{U}U, P_r] + \Pi_s(\dot{P}) \\ &= [P_r, P_s] + \Pi_s(\Delta_N^{-1}[P_r, \Delta_N(P_s + P_r)]), \end{aligned}$$

and

$$\dot{P}_r = -[P_r, P_s] + \Pi_r(\Delta_N^{-1}[P_r, \Delta_N(P_s + P_r)]).$$

To understand how the dynamics of the  $P_s, P_r$  variables look, we consider the first numerical simulation of Section 4. In Figure 8 the three stream function fields  $P, P_s, P_r$  are shown at the times  $t = t_0$  and  $t = t_{end}$ . We notice that from a very smooth  $P$ , the projection  $\Pi_s$  onto the stabilizer rougher field  $W$  produce a much coarser image. In particular, both  $P_s$  and  $P_r$  do not show any additional structure or scale separation unlike to  $W_s$  and  $W_r$ .

## References

- [1] R. V. Abramov and A. J. Majda, Statistically relevant conserved quantities for truncated quasigeostrophic flow, *Proc. Nat. Acad. Sci. (USA)* **100** (2003), 3841–3846.
- [2] G. Boffetta and R. E. Ecke, Two-dimensional turbulence, *Annual Review of Fluid Mechanics* **44** (2012), 427–451.
- [3] M. Bordemann, E. Meinrenken, and M. Schlichenmaier, Toeplitz quantization of Kähler manifolds and  $\text{gl}(n), n \rightarrow \infty$  limits, *Comm. Math. Phys.* **165** (1994), 281–296.
- [4] M. Chertkov, C. Connaughton, I. Kolokolov, and V. Lebedev, Dynamics of energy condensation in two-dimensional turbulence, *Phys. Rev. Lett.* **99** (2007), 084501.

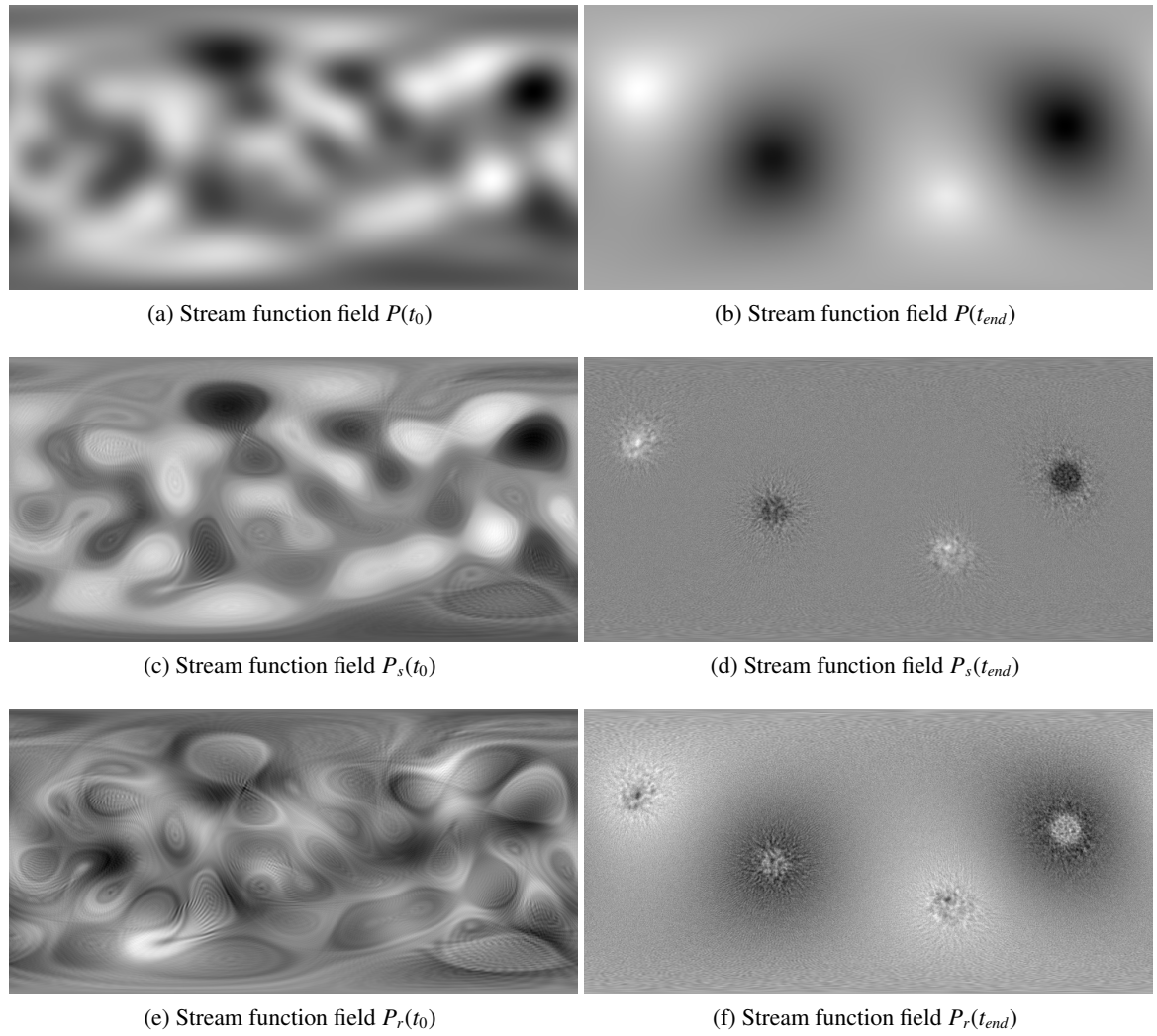


Figure 8: The Stream function fields fields  $P, P_s, P_r$  at  $t = t_0$  and  $t = t_{end}$ .

- [5] D. Dritschel, W. Qi, and J. Marston, On the late-time behaviour of a bounded, inviscid two-dimensional flow, *J. Fluid Mech.* **783** (2015), 1–22.
- [6] M. Farge, K. Schneider, and N. Kevlahan, Non-gaussianity and coherent vortex simulation for two-dimensional turbulence using an adaptive orthogonal wavelet basis, *Physics of Fluids* **11** (1999), 2187–2201.
- [7] E. Hairer, C. Lubich, and G. Wanner, *Geometric Numerical Integration*, second ed., Springer-Verlag, Berlin, 2006.
- [8] C. Herbert, Additional invariants and statistical equilibria for the 2d euler equations on a spherical domain, *Journal of Statistical Physics* **152** (2013).
- [9] J. Hoppe and S.-T. Yau, Some properties of matrix harmonics on  $S^2$ , *Comm. Math. Phys.* **195** (1998), 66–77.
- [10] A. Jain, I. Timofeyev, and E. Vanden-Eijnden, Stochastic mode-reduction in models with conservative fast sub-systems, *Commun. Math. Sci.* **2** (2015), 297–314.
- [11] R. H. Kraichnan, Inertial ranges in two-dimensional turbulence, *Phys. Fluid.* **10** (1967), 1417–1423.
- [12] R. H. Kraichnan and D. Montgomery, Two-dimensional turbulence, *Rep. Prog. Phys.* **43** (1980).
- [13] C. Marchioro and M. Pulvirenti, *Mathematical Theory of Incompressible Nonviscous Fluids*, first ed., Springer-Verlag, New York, 1994.
- [14] R. McLachlan, Explicit Lie–Poisson integration and the Euler equations, *Phys. Rev. Lett.* **71** (1993), 3043–3046.
- [15] K. Modin and M. Viviani, A Casimir preserving scheme for long-time simulation of spherical ideal hydrodynamics, *J. Fluid Mech.* **884** (2020), A22.
- [16] L. Onsager, Statistical hydrodynamics, *Il Nuovo Cimento (1943-1954)* **6** (1949), 279–287.
- [17] M. A. Rutgers, Forced 2d turbulence: Experimental evidence of simultaneous inverse energy and forward enstrophy cascades, *Phys. Rev. Lett.* **81** (1998), 2244–2247.
- [18] V. Zeitlin, Finite-mode analogues of 2D ideal hydrodynamics: Coadjoint orbits and local canonical structure, *Physica D* **49** (1991), 353–362.

- [19] V. Zeitlin, Self-consistent-mode approximation for the hydrodynamics of an incompressible fluid on non rotating and rotating spheres, *Phys. Rev. Lett.* **93** (2004), 353–362.